CHEMISTRY
A EUROPEAN JOURNAL

Effect of Axial Ligation or π–π-Type Interactions on Photochemical Charge Stabilization in "Two-Point" Bound Supramolecular Porphyrin–Fullerene Conjugates

Francis D'Souza,*[a] Raghu Chitta,[a] Suresh Gadde,[a] Melvin E. Zandler,[a] Amy L. McCarty,[a] Atula S. D. Sandanayaka,[b] Yasuyaki Araki,[b] and Osamu Ito*[b]

Abstract: Two types of structurally well-defined, self-assembled zinc porphyrin–fullerene conjugates were formed by "two-point" binding strategies to probe the effect of axial ligation or π–π-type interactions on the photochemical charge stabilization in the supramolecular dyads. To achieve this, *meso*-tetraphenylporphyrin was functionalized to possess one or four [18]crown-6 moieties at different locations on the porphyrin macrocycle while fullerene was functionalized to possess an alkyl ammonium cation, and a pyridine or phenyl entities. As a result of the crown ether–ammonium cation complexation, and zinc–pyridine coordination or π–π-type interactions, stable zinc porphyrin–fullerene conjugates with defined distance and orientation were formed. Evidence for the zinc–pyridine complexation or π–π-type interactions was obtained from the spectral and computational studies. Steady-state and time-resolved emission studies revealed efficient quenching of the zinc–porphyrin singlet excited state in these dyads, and the measured rates of charge separation, k_{CS} were found to be slightly better in the case of the dyads held by axial coordination and crown ether–cation complexation. Nanosecond transient absorption studies provided evidence for the electron transfer reactions, and these studies also revealed charge stabilization in these dyads. The lifetimes of the radical ion pairs were found to depend upon the type of porphyrins utilized to form the dyads, that is, porphyrin possessing the crown ether moiety at the *ortho* position of one of the phenyl rings yielded prolonged charge stabilized states. Addition of pyridine to the supramolecular dyads eliminated the zinc–pyridine coordination or π–π-type interactions of the "two-point" bound systems due to the formation of a new zinc–pyridine axial bond thus giving a unique opportunity to probe the effect of axial coordination or π–π interactions on k_{CS} and k_{CR}. Under these conditions, the measured electron transfer rates revealed faster k_{CS} and slower k_{CR} as compared to those obtained in the absence of added pyridine. The evaluated lifetimes of the radical ion-pairs were found to be hundreds of nanoseconds and were longer in the presence of pyridine.

Keywords: electron transfer · fullerenes · photochemistry · porphyrinoids · supramolecular chemistry

Introduction

Study of photoinduced electron transfer in donor–acceptor dyads is a topic of current interest mainly to address the mechanistic details of electron transfer in chemistry and biology, to develop artificial photosynthetic systems for light energy harvesting,[1–8] and also, to develop molecular optoelectronic devices.[9] Fullerenes as electron acceptors[10] and porphyrins as electron donors[11] have been successfully utilized in the construction of such dyads[12] owing to their rich and well-understood electrochemical, optical, and photochemical properties. Fullerenes, because of their unique structure and symmetry, require small reorganization energy in electron transfer reactions.[13] As a consequence, fuller-

[a] Prof. F. D'Souza, R. Chitta, S. Gadde, Prof. M. E. Zandler, A. L. McCarty
Department of Chemistry, Wichita State University
1845 Fairmount, Wichita, KS 67260-0051 (USA)
Fax: (+1) 316 978-3431
E-mail: Francis.DSouza@wichita.edu

[b] A. S. D. Sandanayaka, Dr. Y. Araki, Prof. O. Ito
Institute of Multidisciplinary Research for Advanced Materials
Tohoku University
Katahira, Sendai, 980-8577 (Japan)
Fax: (+81) 22-217-5610
E-mail: ito@tagen.tohoku.ac.jp

Supporting information for this article is available on the WWW under http://www.chemeurj.org/ or from the author.

DOI: 10.1002/chem.200500186

enes (C_{60} and C_{70}) in donor–acceptor dyads accelerate forward electron transfer (k_{CS}) and slow down backward electron transfer (k_{CR}) resulting in the formation of long-lived charge-separated states, as verified in a number of porphyrin–fullerene dyads.[12] More recently, elegantly designed porphyrin and fullerene bearing molecular and supramolecular triads, tetrads, pentads and so on, have also been synthesized and studied.[14] In some of these supramolecular systems, distinctly separated donor–acceptor radical ion-pairs are generated in succession by charge migration reactions along the well-tuned redox gradients.[14]

Recent studies have revealed the importance of intra- and intermolecular type interactions on the photochemistry of flexibly and rigidly linked molecular and supramolecular porphyrin–fullerene conjugates.[15,16] Information was obtained primarily from the crystal structures of inter- and intramolecularly interacting porphyrin/fullerene conjugates;[17] thus, attempts have been made to model the organization principles and to probe their impact on electron transfer reactions.[12–16] These attempts have led to the development of a variety of porphyrin/fullerene hybrids that give rise to different topologies and chromophore separations. Most of the synthetic methodologies are based on connecting porphyrins and fullerenes by a single linker that resulted in a substantial degree of conformational flexibility in the molecular topology. As a result, the porphyrin/fullerene organization in the resulting hybrids was poorly defined and the fullerene could not be positioned close or on top of the porphyrinic macrocycle. In a few synthetic approaches, the porphyrins and fullerenes were brought together by two separate linkers, yielding dyads with π-stacked sandwich structures. Control over the interchromophore interactions and fine-tuning of the properties of the ground and excited states were possible to some extent by this approach by varying the linker lengths.[18]

Our interest in this area of research has been to utilize multiple modes of binding in a self-assembly process to form rigidly held porphyrin–fullerene conjugates and to visualize the effects of inter- and intramolecular interactions on the physico-chemical properties of these novel supramolecular systems.[19] This approach has provided information about the structure and orientation of the donor–acceptor pair, and minimized the different degrees of electronic coupling due to the different wave function mixing, observed in flexibly linked donor–acceptor pairs. In subsequent studies, the self-assembly approach was also extended to form supramolecular triads bearing three photo/redox active entities, and dyads bearing more than one donor or acceptor entities. The photochemical studies of the self-assembled triads resulted in the successful generation of relatively long-lived charge separated species. The multiple modes of binding utilized different types of binding mechanisms.[19] These include: i) a "coordinate-covalent" binding strategy in which the porphyrin–fullerene interactions were probed by a "tail-on" and "tail-off" binding mechanism,[19a] ii) a "coordinate-hydrogen bonding" strategy which led to the formation of stable supramolecular dyads and triads,[19b] iii) a "coordinate–coordinate bonding" approach of obtaining bisporphyrin–fullerene dyad held in a symmetrical fashion,[19c] and iv) a "coordinate-crown ether cation complex" strategy of obtaining stable porphyrin–fullerene conjugates with defined distance and orientation.[19d] In the latter case owing to the higher stability of the supramolecular complex it was possible to investigate the spectral and photochemical properties in more polar solvent such as benzonitrile. It may be mentioned here that in all of above developed multiple binding mechanisms, metal to pyridine axial binding (coordination) was one of the common modes of binding.

In the present study, we have extended the novel approach of "two-point" binding by utilizing porphyrins bearing one or four [18]crown-6 moieties (compounds **1**–**3** in Scheme 1) and fulleropyrrolidine bearing an alkyl ammonium cation and pyridine entities (compound **4** in Scheme 1). As demonstrated recently for porphyrin **1** interacting with fullerene **4**,[19d] stable porphyrin–fullerene conjugate was obtained in which the pyridine unit was axially coordinated to the zinc center of the porphyrin and the ammonium cation was complexed with the crown ether moiety. Compound **2** is newly synthesized to visualize the "two-point" binding in a porphyrin macrocycle in which the crown ether entity is dis-

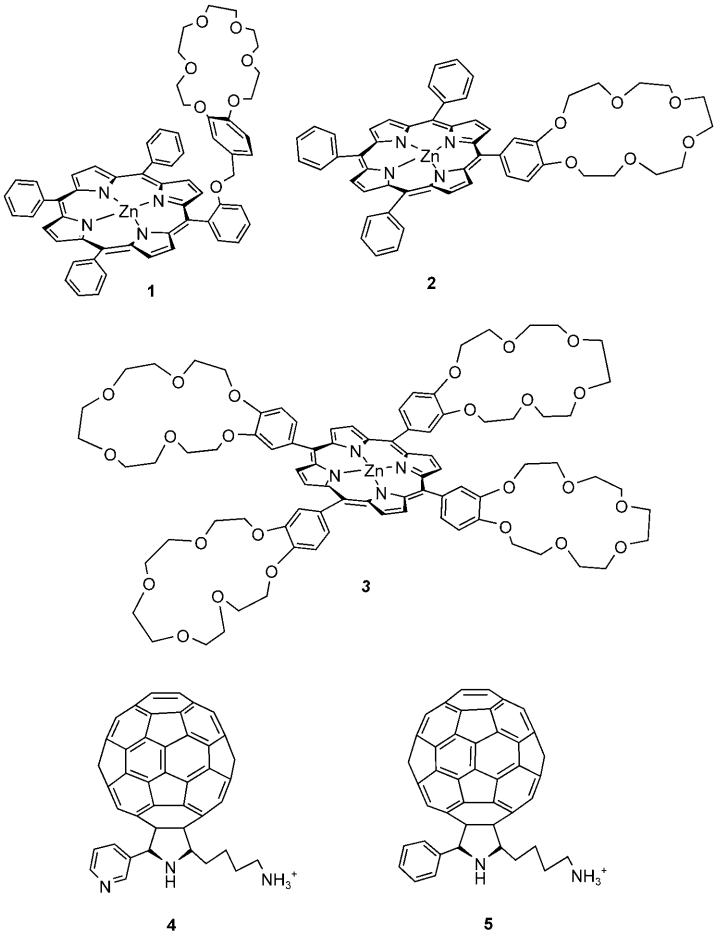

Scheme 1. Structure of the crown ether appended porphyrins and fullerene derivatives employed in the present study.

posed differently than that in **1**, while compound **3** is synthesized to form porphyrin–fullerene conjugates bearing up to four fullerene entities. In order to visualize the π–π-type interactions between the porphyrin–fullerene entities in the self-assembled dyads, fullerene **5** was synthesized which lacks the axial coordinating pyridine unit and has only an alkyl ammonium cation to complex with crown ether. Such fullerene, when bound to a crown ether appended porphyrin, is expected to interact with the porphyrin π-system in addition to the cation–crown ether complexation.[20a] Hence, a comparison of the ground and excited state properties between the "two-point" bound dyads **1**:**4** or **2**:**4**, and the dyads held by only alkyl ammonium cation–crown ether complex, **1**:**5** or **2**:**5** would provide information on the effects of axial ligation versus π–π-type interactions in the presently investigated series of self-assembled dyads on their spectral and photochemical properties. Interestingly, addition of pyridine to these supramolecular compounds eliminates the zinc–pyridine bonds in case of dyads **1**:**4** and **2**:**4**, and the π–π-type interactions in case of dyads **1**:**5** and **2**:**5** as a result of the newly formed zinc-pyridine (externally added) bond (Scheme 2). Photochemical studies under these conditions would provide the role of axial coordination or π–π interactions on the charge separation and charge recombination processes in the supramolecular dyads. These effects have been systematically investigated in the present study.

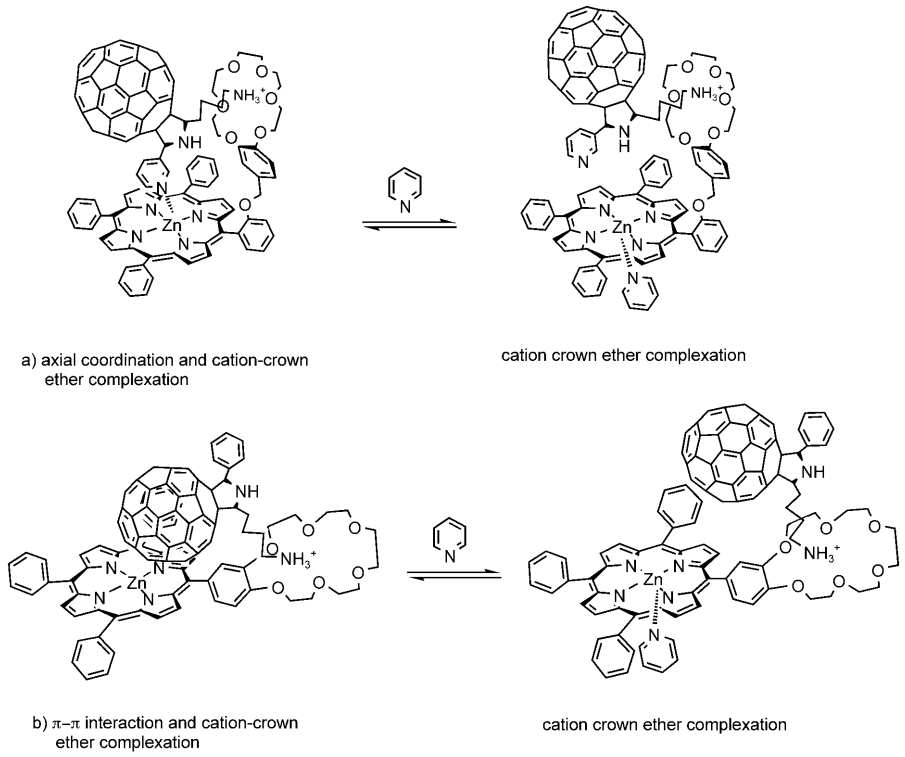

Scheme 2. Effect of external pyridine addition on the structures of the supramolecular dyads.

Results

Optical absorbance studies and ground state interactions: The optical absorption behavior of the benzo-[18]crown-6 appended at different *meso*-positions of the zinc porphyrin macrocycle was found to be similar to that of pristine *meso*-tetraphenylporphyrinatozinc, ZnP. That is, they exhibited an intense Soret band around 425 nm and two visible bands around 560 and 600 nm, respectively. No apparent absorption bands in the wavelength region covering 350–700 nm corresponding to the crown ether entities were observed. Addition of fullerene **4** to a solution containing porphyrin **1** or **2** revealed spectral changes accompanied by one or more isosbestic points. Typical spectral changes are shown in Figure 1 for porphyrin **2** in the presence of increasing amounts of fullerene **4**. The Soret band revealed a decrease in intensity accompanied by a red shift, typical of axial coordination of a nitrogenous ligand. The ^{1}H NMR studies confirmed the "two-point" binding involving axial coordination of the pyridine entity of **4** to the metal center of **1**, and the crown ether-ammonium cation complexation (See Figure S1 in the Supporting Information). The binding constants for zinc porphyrin–fullerene conjugate formation were calculated from Benesi–Hildebrand plots[21] using the absorbance and fluorescence spectral data and the results will be discussed in the subsequent sections.

Interestingly, in the case of fullerene **5** binding to the crown ether appended porphyrins, **1**–**2**, the observed spectral shifts were not so drastic primarily due to the lack of axial coordination. However, spectral evidence for π–π-type interactions between the porphyrin macrocycle and the fullerene spheroid was observed. As shown in Figure 1 inset, a broad band in the 725–825 nm region was observed for the dyad **1**:**5**. Control experiments performed by recording the spectrum of **1**, **5**, and the spectrum obtained by the digital addition of spectrum of **1** and **5** were different in this wavelength region. Earlier, in a number of covalently linked porphyrin–fullerene dyads such broad absorption bands in the 725–900 nm regions were observed as a result of π–π-type interactions.[16,18] A similar but less pronounced spectrum was also observed for the complex **2**:**5** but not for the spectra of **1**:**4** and **2**:**4**. Addition of pyridine to the solution eliminated this spectral band. ^{1}H NMR titrations of fullerene, **5** on increasing addition of porphyrin,

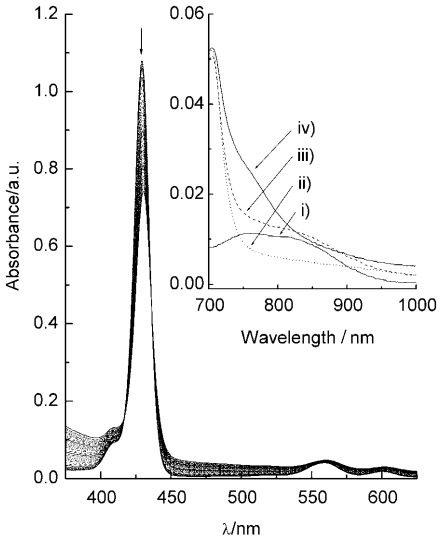

Figure 1. Spectral changes observed during the titration of porphyrin **2** (1.6 μM) with fullerene **4** (0.21 μM each addition) in benzonitrile. The inset shows enlarged near-IR portion of the spectrum for i) porphyrin **1**, ii) fullerene, **5**, iii) digitally added spectrum of i) and ii), and iv) the complex obtained by treating equimolar **1** and **5** in benzonitrile.

1 in $CDCl_3$ revealed systematic high field shift (up to 0.3 ppm) of the pyrrolidine and alkyl protons of the ammonium pendant arm. The shifts of the phenyl ring protons of **5** were found to be <0.1 ppm. The high field shifts were smaller than that earlier reported for the complex **1**:**4** involving both axial coordination and cation–crown ether complexation. The observed high field shift for the dyad **1**:**5** suggests positioning of the fullerene moiety in the ring-current zone of the porphyrin ring with close proximity, that is, the presence of interacting porphyrin and fullerene entities in the complex. To summarize, the present spectral results indicate metal–ligand axial coordination and crown ether–ammonium cation complexation in case of **1**:**4** and **2**:**4**. In the case of **1**:**5** and **2**:**5**, in addition to crown ether–ammonium cation complexation, π–π-type interactions have also been observed.

Ab initio B3LYP/3-21G(*) Computational studies: In order to further understand the geometry and electronic structure of the investigated conjugates, computational studies were performed on all of the investigated dyads by a moderate level ab initio method. Our recent works using the B3LYP/3-21G(*) method on molecular/supramolecular systems have yielded remarkable results not only in predicting the correct geometry but also in predicting π–π-type interactions and tracing the sequence of electrochemical redox processes.[19,22] As a consequence of π–π-type charge transfer interactions in the ground state, partial delocalizations of the HOMO and LUMO frontier orbitals on both the donor and acceptor entities were observed for the donor–acceptor dyads.[16f]

The structures of the self-assembled dyads are shown in Figures 2 and 3a, and the key geometric parameters are given in Table 1. For geometry optimization, the starting porphyrin and fullerene entities were initially optimized on a Born–Oppenheimer potential energy surface and then allowed to interact. The optimized structures of dyads **1**:**4** and **2**:**4** revealed the expected "two-point" binding, namely, zinc–pyridine coordination and crown ether–ammonium cation complex formation. The Zn–N distance of the newly formed coordinate bond was around 2.1 Å which was close to the other four Zn−N bond lengths of the zinc porphyrin. The Zn was pulled out of the porphyrin plane by about 0.4 Å upon axial bond formation. Two sets of N−O distances, 2.80 and 3.00 Å, were observed for the ammonium cation-crown ether complexation. That is, the presence of three sets of N−H···O type hydrogen bonds was visualized. Because of the different position of the crown ether moieties on the porphyrin macrocycle, the topology of the dyads was different, as shown in Figure 2a and b. It may be mentioned here that the porphyrin macrocycle in **1** was distorted considerably upon self-assembling the fullerene while such macrocycle distortions were not found in porphyrin **2**. Interestingly, the center-to-center distance between the zinc–porphyrin and fullerene entities was found to be almost the same, slightly larger than 10 Å. The edge-to-edge distance, that is, the distance between the closest porphyrin π-ring atom to the fullerene spheroid carbon atom was over 4.5 Å, larger than that would be expected to observe any through-space π–π-type interactions. These results suggest that, although dyads **1**:**4** and **2**:**4** have considerable rigidity because of the employed "two-point" binding motif, they have no through space π–π type charge-transfer interactions. These observations readily agree with the earlier discussed optical absorption spectral results.

In contrast to the above results on **1**:**4** and **2**:**4** dyads, the structure of dyads **1**:**5** and **2**:**5** revealed the presence of π–π-type interactions. As shown in Figure 2c for the dyad **1**:**5** and in Figure 3a for the dyad **2**:**5**, the geometric parameters revealed the expected crown ether–ammonium cation complex formation. The calculated center-to-center distances between the porphyrin and fullerene entities were found to be in the range of 5.6 to 6.1 Å while the edge-to-edge distances were in the rage of 2.2 to 2.3 Å (Table 1) indicating closely interacting porphyrin and fullerene entities. It may be mentioned here that slightly energy demanding, "extended type" conformers were possible for **1**:**5** and **2**:**5** dyads. Interestingly, addition of pyridine to form a pentacoordinated zinc porphyrin of the **2**:**5** dyad (Figure 2d), pushed the fullerene entity away from the porphyrin macrocycle by ~1 Å thus eliminating the through space interactions.

The frontier HOMO and LUMO orbitals also revealed the existence of π–π type interactions in these dyads. As shown in Figure 3b and c for the dyad **2**:**5**, considerable amounts of HOMO were found on the fullerene entity, while part of LUMO was also found on the porphyrin entity of the dyad. Similar results of delocalization of the frontier orbitals were observed for the studied dyad **1**:**5** but not for the dyads **1**:**4** and **2**:**4**. It may also be mentioned here that the dyad **2**:**5** in the presence of pyridine bound to zinc did

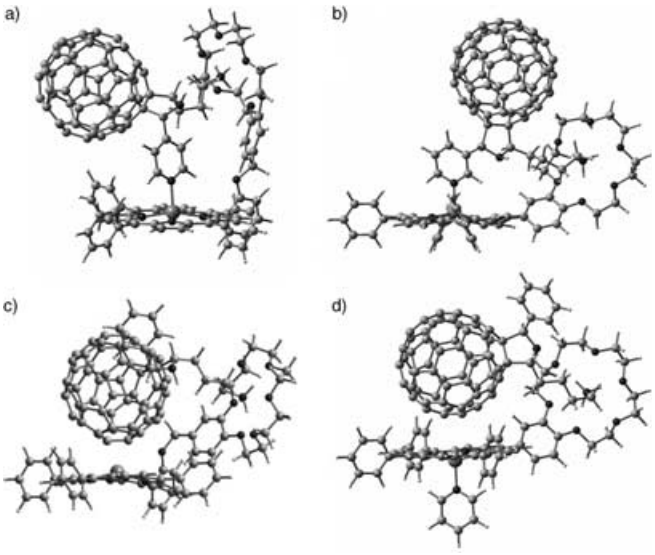

Figure 2. Ab initio B3LYP/3-21G(*) calculated structures of the self-assembled dyads a) **1**:**4**, b) **2**:**4**, c) **1**:**5** and d) **2**:**5** with pyridine axial ligand.

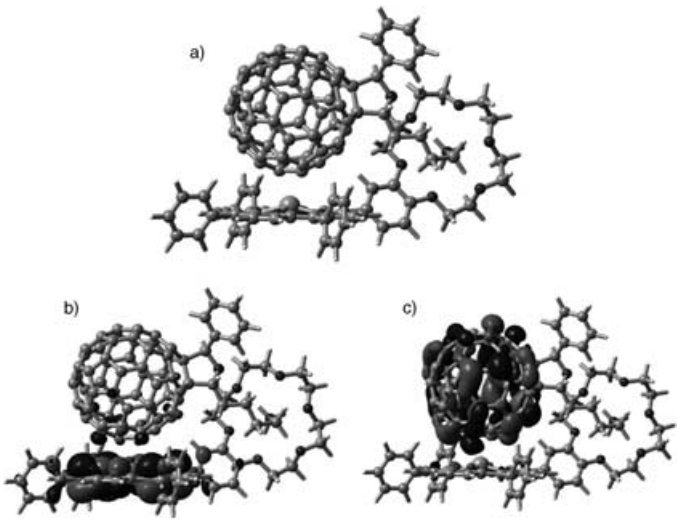

Figure 3. Ab initio B3LYP/3-21G(*) calculated a) optimized structure, b) HOMO, and c) LUMO of the self-assembled **2**:**5** dyad.

Table 1. B3LYP/3-21G(*) optimized geometric parameters for the crown-ether-ammonium cation complexed, self-assembled zinc porphyrin–fullerene conjugates.

Dyad[a]	center-to-center Distance [Å][b]			edge-to-edge Distance [Å]
	ZnP-C_{60}	ZnP-N	C_{60}-N	ZnP-C_{60}
1:**4**	10.1	10.1	10.2	4.5
2:**4**	10.7	9.7	8.7	6.7
1:**5**	6.1	10.6	9.2	2.3
2:**5**	5.6	10.2	10.0	2.2
Py:**2**:**5**[c]	6.7	10.5	10.0	3.3

[a] See Scheme 1 for structures. [b] Zinc metal center, center of C_{60} spheroid, and N of ammonium cation were used. [c] Axial coordination of pyridine to the zinc center, see Figure 2d.

not reveal such delocalization of the frontier orbitals correlating with the increased distance between the entities.

Fluorescence emission studies: The singlet excited-state quenching of crown ether appended porphyrins by functionalized fullerenes was investigated to obtain the binding constants of the self-assembled dyads and the overall fluorescence quenching behavior with respect to differently assembled zinc porphyrin–fullerene dyads. The emission behavior of the crown ether appended porphyrins was found to be similar to that of ZnP with two emission bands around 610 and 660 nm, respectively. Addition of either of the fullerene derivatives, **4** or **5**, to a solution of either of porphyrins **1**, **2**, or **3**, revealed fluorescence quenching in benzonitrile. Representative emission changes of **2** on increasing addition of **4** are shown in Figure 4. By using the emission data, the binding constants (K) for the formation of self-assembled dyads were obtained by constructing Benesi–Hildebrand plots[21] (Figure 4, inset), and the data are listed in Table 2. The magnitude of the binding constants revealed stable self-assembly in polar benzonitrile and agreed well with that reported on **1**:**4** by using absorbance methods.[19d] Earlier, for the "one-point" bound through axial coordinating zinc porphyrin–fullerene dyads,[22c] it was not possible to perform spectroscopic studies in polar benzonitrile signifying the importance of the adopted "two-point" binding strategy in the present study. For porphyrin **1**, the binding of **4** is 2–3 times larger than that of **5**. Similarly, for porphyrin **2**, the binding of **4** is an order of magnitude higher than that of **5**. This could be rationalized based on the ability of **4** to form "two-point"

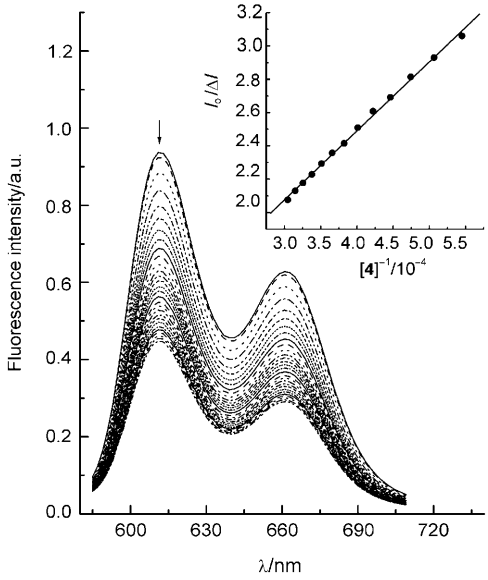

Figure 4. Fluorescence spectral changes observed on increasing addition of fullerene **4** (2.0 μM each addition) to a solution of porphyrin **2** in benzonitrile. $\lambda_{ex} = 560$ nm. The inset shows the Benesi–Hildebrand plot at 615 nm constructed for measuring the binding constant; I_o (fluorescence intensity in the absence of **4**), and ΔI (changes of fluorescence intensity on addition of **4**).

Table 2. Formation constants calculated from the Benesi–Hildebrand plots of the fluorescence data for the "two-point" bound zinc porphyrin–fullerene conjugates in benzonitrile at 25 °C.

Porphyrin Receptor[a]	Fullerene	K [M^{-1}][b]
1	**4**	4.48×10^4
	5	1.64×10^4
2	**4**	2.08×10^4
	5	1.30×10^3
3[c]	**5**	4.80×10^3

[a] See Scheme 1 for structures of the porphyrin and fullerene derivatives. [b] Error = ±10%. [c] Overall binding constant.

binding involving axial ligation and crown ether-cation complex formation. The smaller K values of **1**:**5** and **2**:**5** suggest that the contributions from the π–π-type interactions are smaller than the axial coordination bond of dyads **1**:**4** and **2**:**4**. However, it may be mentioned here that the π–π-type interactions indeed contribute to the overall stability of the self-assembled dyads.

Figure 5 shows the Stern–Volmer plots of the fluorescence quenching by the crown ether appended porphyrins by the functionalized fullerenes. The slope of the plots followed the binding constants, that is, the efficiency of fluorescence quenching was higher for more stable complexes. The calculated Stern–Volmer constant, K_{SV} values were found to range between $1.2\times10^3\,M^{-1}$ and $1.6\times10^5\,M^{-1}$. On employing the excited state lifetime of zinc porphyrin to be 2 ns, the fluorescence quenching rate-constants, k_q, were two to four orders of magnitude higher than that expected for diffusion controlled-bimolecular quenching processes in benzonitrile ($5.0\times10^9\,M^{-1}s^{-1}$) suggesting that the intramolecular processes are responsible for the fluorescence quenching. The tendency of increasing in the k_q values is in good agreement with those evaluated K values.

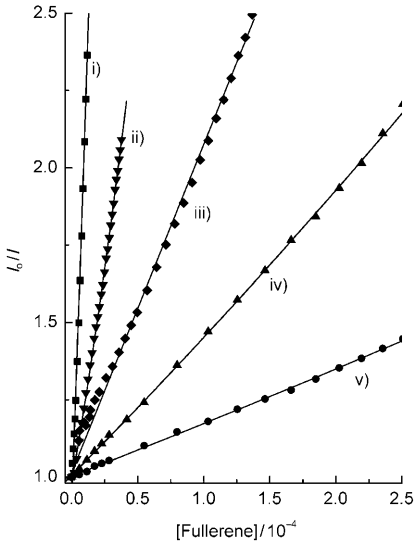

Figure 5. Stern–Volmer plots of fluorescence quenching at 616 nm of i) **1** by **4**, ii) **2** by **4**, iii) **1** by **5**, iv) **3** by **5**, and v) **2** by **5** in benzonitrile, λ_{ex} = 558 nm.

Scanning the emission wavelength of the zinc porphyrin–fullerene dyads to longer wavelength regions (700–800 nm) revealed a weak emission band around 715 nm corresponding to the singlet emission of the C_{60} moiety. The intensity of this band for a given concentration of fulleropyrrolidine was found to be almost the same as that obtained in the absence of added zinc porphyrin. Changing the excitation wavelength from 560 to 410 nm also revealed similar observations with slightly enhanced emission of fulleropyrrolidine due to its higher absorbance at 410 nm. These results suggest that emission in the 700–800 nm range is attributable to direct excitation of the fullerene unit.

Electrochemical studies: Cyclic voltammetric studies were performed to evaluate the redox potentials of the dyads. The zinc porphyrins, **1** and **2** revealed two one-electron oxidations corresponding to the formation of $ZnP^{\bullet+}$ and ZnP^{2+}, respectively (Figure 6), and a one-electron reduction corresponding to the formation of $ZnP^{\bullet-}$. Scanning the potential further in the negative direction revealed another reduction but was not well defined. Upon forming the dyads, the oxidation waves revealed interesting changes. That is, the first oxidation processes were still reversible but were easier to oxidize by 5–30 mV, depending upon the nature of the porphyrin and the fullerene. The first oxidation processes of ZnP in the dyads were located in the range 0.27–0.30 V versus Fc/Fc^+. Such cathodic shifts were much more pronounced for the second oxidation processes. That is, shifts in the range of 30–100 mV were observed. However, the second oxidation processes were found to be irreversible. In these dyads, the potentials corresponding to the reductions of fulleropyrrolidine were not different from that of unbound fulleropyrrolidine.[22c] The first reduction of fulleropyrrolidine in the dyads was located at $E_{1/2} = -1.10$ V versus Fc/Fc^+ (data not shown). The free-energy changes for charge separation, ΔG_{CS} and charge recombination, ΔG_{CR} were calculated by using the first oxidation potential of ZnP, the first reduction potential of fulleropyrrolidine, singlet excitation energy of the ZnP, and the Coulomb energy according to Weller's approach.[23] Both ΔG_{CS} and ΔG_{CR} were found to be exothermic with values ranging between −0.70 to −0.72 eV for ΔG_{CS} and −1.31 to −1.33 eV for ΔG_{CR}. These negative ΔG_{CS} values indicate that the charge-separation process is probably near the top region of the Marcus parabola, because the reported reorganization energy (about 0.7 eV)[14d] is almost the same as the absolute value of ΔG_{CS}. On the other hand, the ΔG_{CR} values suggest that the charge-recombination process belongs to the inverted region of the Marcus parabola.[14d]

Further, time-resolved emission and transient absorption studies were performed to follow the kinetics of quenching and to characterize the photo reaction products.

Pico-second time-resolved emission studies: The time-resolved emission studies of the self-assembled dyads tracked those of steady-state measurements. Figure 7a–c show the emission decay time profile of the crown ether appended

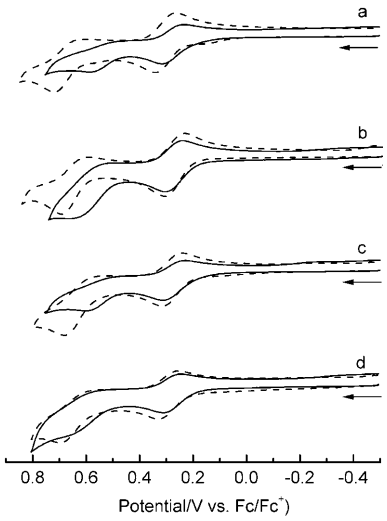

Figure 6. Cyclic voltammograms showing the oxidation processes of a) **1** in the absence (-----) and presence (——) of 1 equiv **4**, b) **1** in the absence (dashed line) and presence (——) of 1 equiv **5**, c) **2** in the absence (-----) and presence (——) of 1 equiv **4**, and d) **2** in the absence (-----) and presence (——) of 1 equiv **5** in benzonitrile, 0.1 M $(n\text{-}C_4H_9)_4NClO_4$. Scan rate = 100 mV s^{-1}.

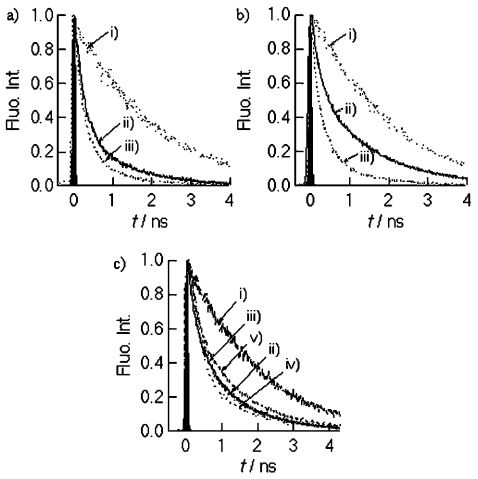

Figure 7. a) Fluorescence decays at 610–630 nm of i) porphyrin **1** (0.1 mM), ii) porphyrin **1** (0.1 mM) in the presence of fullerene **5** (0.15 mM) and iii) porphyrin **1** (0.1 mM) in the presence of fullerene **4** (0.15 mM) in benzonitrile. b) Fluorescence decays of i) porphyrin **2** (0.1 mM), ii) porphyrin **2** (0.1 mM) in the presence of fullerene **5** (0.15 mM) and iii) porphyrin **2** (0.1 mM) in the presence of fullerene **4** (0.15 mM) in benzonitrile. c) Fluorescence decays of porphyrin **3** (0.1 mM), in the presence of i) 0.0 mM, ii) 0.11 mM, iii) 0.21 mM, iv) 0.31 mM and v) 0.42 mM) of fullerene **5** in benzonitrile. All of the samples were excited at 410 nm.

porphyrins, **1**–**3** in the absence and presence of fullerene derivatives, **4** and **5**. The lifetimes of the singlet excited crown ether appended porphyrins were found to be similar to that of ZnP, around 2 ns, and all of them revealed mono-exponential decay. The appended crown ether moieties had little or no influence on the lifetime of the porphyrin. Addition of 1.5 equivalents of fullerene derivatives to ensure complete complexation of the porphyrins (**1** or **2**) caused rapid decay in addition to slow decaying tail as shown in Figure 7. The porphyrin emission decay in the dyads could be fitted satisfactorily by a bi-exponential decay curve; the lifetimes (τ_f) are summarized in Table 3. The fractions of the short τ_f components seem to increase with the K values in Table 2, the slow τ_f components may be related to the uncomplexed porphyrin emission.

Based on the observations that the time resolved fluorescence spectra did not show the appearance of the transient fluorescence peak of the C_{60} moiety after the decay of the fluorescence of the ZnP moiety, the short lifetimes of ZnP are predominantly due to charge-separation within the supramolecular dyads. Thus, the charge-separated rates (k_{CS}^S) and quantum yields (Φ_{CS}^S) were evaluated from the short τ_f components in the usual manner employed in the intramolecular electron-transfer process,[19] as listed in Table 3. Higher values of k_{CS}^S and Φ_{CS}^S were obtained for all of the dyads indicating the occurrence of efficient electron transfer irrespective of the nature of the adopted binding modes. The k_{CS}^S values are generally higher for the "two-point" bound system involving axial coordina-

Table 3. Fluorescence lifetime (τ_f), charge-separation rate-constant (k_{CS}^S),[a] charge-separation quantum yield (Φ_{CS}^S)[b], charge-recombination rate constant (k_{CR}) and lifetime of the radical ion-pair for the investigated zinc porphyrin–fullerene conjugates in benzonitrile.

Porphyrin	Fullerene	τ_f [ps] (%)	k_{CS}^S [s^{-1}]	Φ_{CS}^S	k_{CR} [s^{-1}]	τ_{RIP} [ns]
1		1980 (100)				
1	**4**	280 (83) 1180 (17)	3.1×10^9	0.86	2.1×10^7	50
1	**5**	330 (82) 1270 (18)	2.6×10^9	0.84	1.0×10^7	100
Py:**1**[c]	**4**	280 (79) 1560 (21)	3.0×10^9	0.86	4.0×10^6	250
Py:**1**	**5**	300 (80) 1640 (20)	2.8×10^9	0.85	3.6×10^6	280
2		1960 (100)				
2	**4**	300 (80) 1460 (20)	2.8×10^9	0.85	4.7×10^6	210
2	**5**	320 (57) 1520 (43)	2.6×10^9	0.84	4.9×10^6	200
Py:**2**[c]	**4**	300 (82) 1420 (18)	2.9×10^9	0.85	2.0×10^6	500
Py:**2**	**5**	300 (50) 1450 (50)	2.8×10^9	0.84	2.6×10^6	390
3		1950 (100)				
3	**5**	370 (65) 1500 (35)	2.2×10^9	0.82	1.2×10^7	80

[a] $k_{CS}^S = (1/\tau_f)_{complex} - (1/\tau_f)_{ZnP}$. [b] $\Phi_{CS}^S = [(1/\tau_f)_{complex} - (1/\tau_f)_{ZnP}]/(1/\tau_f)_{complex}$. [c] In pyridine (0.1 mM).

tion and crown ether-cation complexation than that involving crown ether-cation complexation and π–π interactions. It may also be mentioned here that the magnitudes of k_{CS}^{S} and Φ_{CS}^{S} are close to those reported earlier for a number of covalently linked zinc porphyrin–fullerene dyads.[15,16] Nanosecond transient absorption spectral studies were also performed to characterize the electron transfer products.

Nanosecond transient absorption studies: Transient spectra recorded after 550 nm laser irradiation of crown ether appended porphyrins, **1–3** revealed absorption peaks at 630 and 840 nm corresponding to the excited triplet state of zinc porphyrin.[25] Fullerenes **4** and **5** showed a band at 700 nm corresponding to their excited triplet state.[25a] It may be mentioned here that the 550 nm laser did not cause decomposition of the crown ether appended porphyrins under the present experimental conditions. Figure 8 shows the transient absorption spectra of **1**:**4** at different time-intervals for the studied self-assembled zinc porphyrin–fullerene dyads. Transient spectra of other studied supramolecular dyads are given in the Supporting Information. In these spectra, in addition to the peaks corresponding to the triplet excited zinc porphyrin and fullerene, peaks at 600 nm corresponding to the formation of zinc porphyrin cation radical and at 1020 nm corresponding to the formation of fulleropyrrolidine anion radical were observed. These spectral features provide experimental proof for the assigned electron transfer fluorescence quenching mechanism.

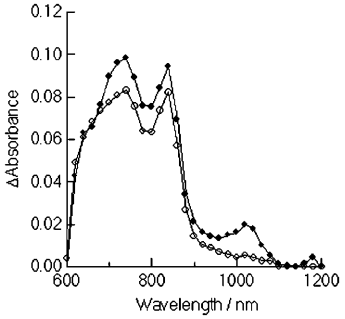

Figure 8. Nanosecond transient absorption spectra of porphyrin **1** (0.1 mM) in the presence of fullerene **4** (0.11 mM, at 32 ns (●) and 320 ns (○) after the 550 nm laser irradiation in benzonitrile.

In order to calculate the rate of charge recombination k_{CR}, the decay of the fulleropyrrolidine anion radical peak at 1020 nm was monitored. As shown in Figure 9, the time profile at 1020 nm followed the first-order decay suggesting the occurrence of intramolecular charge recombination process of the radical ion-pair. The k_{CR} values thus measured in Table 3 are 2–3 orders of magnitude smaller than k_{CS} suggesting charge stabilization in the dyads. The lifetimes of the radial ion-pairs, τ_{RIP} were evaluated from the k_{CR} as given in Table 3. The magnitude of the τ_{RIP} values was found to range between 50–210 ns suggesting that the charge stabilization in these dyads depends upon the nature of the porphyrin and the resulting complex. That is, the charge stabilization is generally higher for dyads formed from porphyrin **2** than from porphyrin **1**. The τ_{RIP} value for the **1**:**4** complex is shorter than that for the **1**:**5** complex indicating that the charge recombination tends to be accelerated via the coordination bond of **1**:**4** more than the π–π interactions (through-space) of **1**:**5**. This could be reasonably explained because of the longer distance between the ZnP and C_{60} entities of the **1**:**4** complex (Table 1). On the other hand, the τ_{RIP} value for **2**:**4** is almost the same as that of **2**:**5**, suggesting that the charge-recombination via π–π interactions (through-space) is preferred over the coordination bond, because of the shorter distance between the ZnP and C_{60} entities. Interestingly, complexes formed from porphyrin **3** bearing up to four fullerene entities had no additional effect in terms of slowing down the charge-recombination process. Additionally, the fast rise of the 1020 nm band also suggests that the charge separation from the triplet excited states is a minor contributor to the overall electron transfer process.

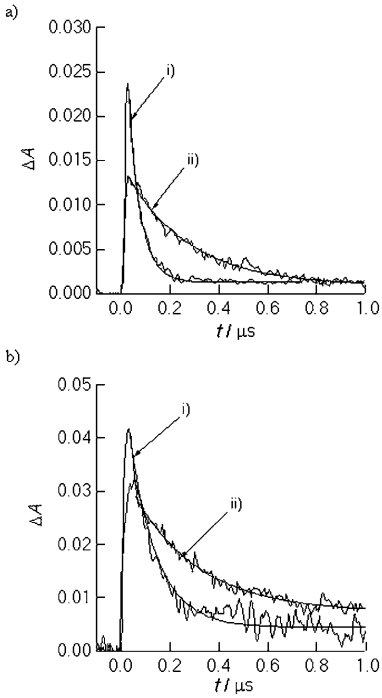

Figure 9. Absorption time profiles of a) i) porphyrin **1** (0.10 mM) in the presence of fullerene **4** (0.11 mM), ii) porphyrin **1** (0.10 mM) in the presence of fullerene **4** (0.14 mM) and pyridine (0.11 mM) at 1020 nm in PhCN; b) i) porphyrin **1** (0.10 mM) in the presence of fullerene **5** (0.11 mM), ii) porphyrin **1** (0.10 mM) in the presence of fullerene **5** (0.14 mM) and pyridine (0.11 mM) at 1020 nm in benzonitrile.

Pyridine complexation to zinc porphyrin—Retro axial coordination or π–π interaction effect: As discussed earlier from optical absorption and computational modeling studies, addition of pyridine to dyads **1**:**4** or **2**:**4** replaces the zinc–pyridine coordination bond of the supramolecular complexes with the formation of a new zinc–pyridine bond (Sche-

me 2a). Similarly, addition of pyridine to the supramolecular complexes of **1**:**5** and **2**:**5** forms a new zinc–pyridine coordination bond and attenuates the π–π interactions (Scheme 2b) yielding increased porphyrin–fullerene distances (Figure 2d and Table 1). Hence, photochemical measurements in the presence of pyridine would give us a unique opportunity to verify the axial coordination and π–π interactions on the rates of charge separation, k_{CS} and rates of charge recombination, k_{CR}. In the case of supramolecular complexes held by axial coordination and cation–crown ether complexation, addition of pyridine would keep the coordination number of the central zinc the same, and therefore the electronic structure of zinc porphyrin would not be significantly different. Only small changes in the donor–acceptor distances would be anticipated. In the case of the complexes held by π–π interactions and cation–crown ether complexation, addition of pyridine would cause slight changes in the redox potentials (<15 mV change), and red shifts of the absorption and emission bands in addition to increased donor–acceptor distances. Importantly, the π–π type interactions observed in **1**:**5** and **2**:**5** are attenuated upon axial coordination as shown in Figure 2d and Table 1.

In general, as listed in Table 3, addition of pyridine to supramolecular dyads slightly increased the k_{CS} values which could easily be attributed to the slightly better donor ability of the zinc–porphyrin upon axial pyridine coordination. The slight increase in the donor–acceptor distance upon axial pyridine coordination had no appreciable effect on k_{CS} or this effect is factored into the observed k_{CS}. Interestingly, the measured k_{CR} revealed slower rates of charge recombination. The lifetimes of the radical ion-pair calculated from the k_{CR} values were found to be hundreds of nanoseconds suggesting longer lifetimes of the charge-separated state upon axial pyridine coordination for both types of supramolecular complexes. That is, elimination of either the axial coordination shown in Scheme 2a or attenuation of π–π interactions as shown in Scheme 2b for the studied supramolecular complexes elongates the distance between ZnP and C_{60}, resulting in slower charge-recombination rates.

Discussion

The results of the present study demonstrate several important points. The design of the "two-point" bound systems involving crown ether–cation complexation and either axial coordination or π–π type interactions has yielded, highly stable, self-assembled zinc porphyrin–fullerene conjugates which allowed us to perform the spectral and photochemical studies in a polar solvent, benzonitrile. This is unlike a number of previous studies on "one-point" bound self-assembled porphyrin–fullerene dyads, where the spectral and photochemical studies could be performed only in nonpolar solvents such as toluene and dichlorobenzene, due to the limited stability of these types of conjugates.[22c,e,f] Because of the adopted "two-point" binding, the dyads revealed defined structure and topology depending upon the position of the crown ether on the porphyrin macrocycle and type of interactions (coordination or π–π-type).

It has been possible to control intramolecular interactions between the donor and acceptor entities by using the present "two-point" binding methodology. By the choice of an axial ligating pyridine entity on the fullerene (compound **4**) or phenyl entity (compound **5**), it was possible to achieve control over axial coordination and π–π interactions. Although the former type of dyads involving axial coordination and crown ether–cation complexation was more stable than the latter type involving π–π interactions and crown ether–cation complexation, computational studies revealed longer distances between the porphyrin and fullerene entities in the former type of dyads compared with the relatively shorter distances of the latter type.

Photochemical studies revealed light induced electron transfer from the singlet excited porphyrin to the fullerene as the main fluorescence quenching mechanism irrespective of the type of binding modes. Both steady-state and time-resolved emission studies revealed efficient fluorescence quenching and the measured rate of charge separation was slightly higher for the dyads formed by axial coordination and crown ether–cation complexation binding mechanism. One possibility for the slightly low k_{CS} values for the dyads involving π–π interactions and crown ether–cation complexation could be due to the existence of "free" and "bound" forms of the π-interacting species. In the "free" form, where only the crown ether–cation complex holds the dyad, the electron donor–acceptor distance would increase considerably (up to 5 Å from computational modeling). Under these conditions, the measured rates could be the average of the different conformers.

Another important aspect is the ability of these self-assembled dyads to stabilize the charge separated states thus creating radical ion-pairs of long lifetimes in the 50–500 ns range. Free-energy calculations revealed that the charge recombination process for these dyads occurs in the inverted region of the Marcus parabola similar to the reported observations for a number of covalently linked and self-assembled porphyrin–fullerene conjugates. However, the measured τ_{RIP} values suggest that the dyads formed from porphyrin **2** are better combinations than porphyrin **1** irrespective of the type of fullerene used to form the dyad. One of the reasons for these findings might involve the differences in the mechanism of the charge-recombination processes; that is, via axial coordination bond versus via through-space π–π interactions.

It was possible to achieve additional charge stabilization by eliminating the zinc–pyridine axial bond or by attenuating π–π interactions by the addition of pyridine to the solution containing the dyads. The measured k_{CS} values were slightly higher and the k_{CR} values were considerably lower in the presence of pyridine. Keeping in mind the small changes in the energetics upon external pyridine coordination, the lower k_{CR} value can be attributed to the increased distance between the porphyrin–fullerene entities as a result of the externally added pyridine coordination. These points

delineate the importance of the present methodology for building stable supramolecular porphyrin–fullerene conjugates with defined distance and orientation, and subsequent manipulation of the rates of electron-transfer by controlling the axial coordination or π–π interactions during photoinduced processes in these novel supramolecular dyads.

Experimental Section

Chemicals: Buckminsterfullerene, C_{60} (+99.95%) was from SES Research (Houston, TX). All the chromatographic materials and solvents were procured from Fisher Scientific and were used as received. Tetra-*n*-butylammonium perchlorate $(n\text{-}C_4H_9)_4NClO_4$ was from Fluka Chemicals. All other chemicals utilized in the synthesis were from Aldrich Chemicals (Milwaukee, WI) and were used as received.

Synthesis of porphyrin and fullerene derivatives

H_2-5-(2-Hydroxyphenyl)-10,15,20-triphenylporphyrin (1a): This compound was synthesized according to the literature procedure.[25] ^{1}H NMR (400 MHz, $CDCl_3$, 25°C, TMS): δ = 8.89–8.84 (m, 8H, β-pyrrolic *H*), 8.23–8.17 (m, 6H, *o*-phenyl *H)*, 8.0–7.96 (dd, 2H, *o,m-H meso*-substituted phenyl), 7.78–7.64 (m, 9H, *m,p*-phenyl *H*), 7.33–7.26 (m, 2H, *m,p-H meso*-substituted phenyl), 5.0 (br s, 1H, OH).

4′-Formylbenzo-[18]crown-6 (1b): This compound was synthesized according to the following procedure: A mixture of 3,4-dihydroxybenzaldehyde (1 g, 7.24 mmol) and excess K_2CO_3 (5.0031 g, 36.2 mmol) taken in DMF (~50 mL) was stirred at ~80°C under nitrogen for 30 min. Then pentaethylene glycol di-*p*-toluene sulfonate (3.483 mL, 7.9641 mmol) was added to the reaction mixture during 20 minutes, and stirred at ~80°C under nitrogen atmosphere for 20 h. The cooled mixture was filtered and the filtrate was evaporated to dryness and the residue was extracted with chloroform. The extract was evaporated to yield a viscous oil which was purified through column chromatography over silica gel by using $CHCl_3$/MeOH 98:2. Evaporation of the solvent yielded a pale-yellow oil, which upon triturating with diethyl ether and refrigeration gave the desired product as a white solid (1.85 mg, ~75%). ^{1}H NMR (400 MHz, $CDCl_3$, 25°C, TMS): δ = 9.84 (s, 1H), 7.44 (dd, 1H, phenyl *H*), 7.39 (d, 1H, phenyl *H)*, 6.95 (d, 1H, phenyl *H)*, 4.28–4.18 (m, 4H, crownethylene *H*), 4.02–3.90 (m, 4H, crownethylene *H*), 3.82–3.71 (m, 8H, crownethylene *H*), 3.69 (s, 4H, crownethylene *H*).

4′-Hydroxymethylbenzo-[18]crown-6 (1c): This compound was obtained by reduction of the above synthesized formyl-derivative, **1b** by using a procedure described by Kryatova et al.[26] 4′-Formylbenzo-[18]crown (**1b**) (1 g, 2.93 mmol) was suspended in absolute ethanol (15 mL), and the mixture was cooled to 0°C. Sodium borohydride (125 mg, 3.3 mmol) was added to this suspension in small portions, maintaining the temperature below 7°C. After the addition of sodium borohydride, the mixture was stirred at 0°C for 2 h and the solvent was rotary evaporated. The residue was washed with water and extracted with CH_2Cl_2 (835 mg, ~85%). ^{1}H NMR (400 MHz, $CDCl_3$, 25°C, TMS): δ = 6.92 (d, 1H, phenyl *H*), 6.88–6.78 (m, 2H, phenyl *H*), 4.60 (s, 2H, benzyl *H*), 4.22–4.06 (m, 4H, crownethylene *H*), 3.98–3.82 (m, 4H, crownethylene *H*), 3.80–3.58 (m, 12H, crownethylene *H*), 2.20 (br s, 1H).

4′-Chloromethylbenzo-[18]crown-6 (1d): This compound was prepared according to Kryatova et al.[26] 4′-Hydroxymethylbenzo-[18]crown-6] (**1c**) (200 mg, 0.59 mmol) was dissolved in CH_2Cl_2 (15 mL), and fine powder of K_2CO_3 (270 mg, 1.954 mmol) was added. The mixture was cooled to 0°C under N_2, and thionyl chloride (96 μL, 1.31 mmol) was added. The reaction was stirred for 1 hour, then filtered and the solvent was evaporated to give a semi-solid product (192 mg, ~90%), which was used without further purification. ^{1}H NMR (400 MHz, $CDCl_3$, 25°C, TMS): δ = 6.92 (m, 2H, phenyl *H)*, 6.82 (d, 1H, phenyl *H)*, 4.55 (s, 2H, benzyl *H)*, 4.24–4.10 (m, 4H, crownethylene *H)*, 4.0–3.84 (m, 4H, crownethylene *H*), 3.80–3.60 (m, 12H, crownethylene *H)*.

H_2-5-(2-Oxomethylbenzo-[18]crown-6-phenyl)-10,15,20-triphenylporphyrin (1e): A mixture of **1a** (335 mg, 0.53 mmol) and excess K_2CO_3 (220 mg, 1.592 mmol) taken in DMF (~50 mL) was stirred at ~80°C under nitrogen for 30 min. Then, 4′-chloromethylbenzo-[18]crown-6 (**1d**) (190 mg, 0.53 mmol) dissolved in minimum amount of DMF was added to the reaction mixture over 20 min, and stirred at ~80°C under nitrogen atmosphere for 18 h. The cooled mixture was filtered and the filtrate was evaporated to dryness and the residue was extracted with chloroform. The extract was evaporated and the residue was subjected to column chromatography over basic alumina. The desired compound was eluted with CH_2Cl_2/EtOAc 80:20 (430 mg, ~85%). ^{1}H NMR (400 MHz, $CDCl_3$, 25°C, TMS): δ = 8.92–8.78 (m, 8H, β-pyrrolic *H*), 8.34–8.12 (m, 6H, *o*-phenyl *H*), 8.05 (dd, 1H, *ortho-H meso*-substituted phenyl), 7.80–7.62 (m, 10H, *m,p*-phenyl *H*), 7.38–7.28 (m, 2H, *m,p*-phenyl *H*), 6.25 (s, 2H, benzocrown-phenyl *H*), 5.18 (s, 1H, benzocrown-phenyl *H*), 4.85 (s, 2H, benzyl *H*), 3.68–3.59 (m, 2H, crownethylene *H*), 3.52–3.48 (m, 2H, crownethylene *H*), 3.47–3.36 (m, 6H, crownethylene *H*), 3.34–3.26 (m, 2H, crownethylene *H*), 3.18–3.08 (m, 2H, crownethylene *H*), 2.58–2.48 (m, 2H, crownethylene *H*), 1.52–1.42 (m, 2H, crownethylene *H*), 1.41–1.32 (m, 2H, crownethylene *H*), −2.7 (br s 2H, imino *H*); UV/Vis (toluene): λ_{max} = 419.0, 514.0, 547.5, 590.0, 645.5 nm.

5-(2-Oxomethylbenzo-[18]crown-6-phenyl)-10,15,20-triphenylporphyrinatozinc(II) (1): The free-base porphyrin **1e** (100 mg, 0.105 mmol) was dissolved in $CHCl_3$ (20 mL), a saturated solution of zinc acetate in methanol was added to the solution, and the resulting mixture was refluxed for 2 h. The course of the reaction was followed spectrophotometrically by the disappearance of the 514.0 nm band of **1e**. At the end, the reaction mixture was washed with water and dried over anhydrous Na_2SO_4. Chromatography on basic alumina by using $CHCl_3$/EtOAc 80:20 gave the title compound (96 mg, ~90%). ^{1}H NMR (400 MHz, $CDCl_3$, 25°C, TMS): δ = 8.86–8.74 (m, 8H, β-pyrrolic *H*), 8.14–8.0 (m, 6H, *o*-phenyl *H*), 7.78 (dd, 1H, *ortho-H meso*-substituted phenyl), 7.73–7.57 (m, 10H, *m,p*-phenyl*H*), 7.31–7.17 (m, 2H, *m,p*-phenyl *H*), 6.23–6.15 (m, 1H, benzocrown-phenyl *H*), 5.91 (d, 1H, benzocrown-phenyl *H*), 4.99 (m, 1H, benzocrown-phenyl *H*), 4.81 (s, 2H, benzyl *H*), 3.08–2.92 (m, 2H, crownethylene *H*), 2.65–2.40 (m, 8H, crownethylene *H*), 2.32–2.2 (m, 2H, crownethylene *H*), 1.72–1.62 (m, 2H, crownethylene *H*), 1.2–1.1 (m, 2H, crownethylene *H*), 1.08–0.98 (m, 2H, crownethylene *H*), 0.76–0.62 (m, 2H, crownethylene *H*); UV/Vis (toluene): λ_{max} = 424.5, 552.0, 592.5 nm; ESI mass in CH_2Cl_2: *m/z*: calcd for: 1018.5; found: 1018.3 $[M]^+$, 1049.2 $[M+MeOH]^+$.

H_2-5-(benzo-[18]crown-6-10,15,20-triphenylporphyrin (2a): A mixture of 4′-formylbenzo-[18]crown-6 (**1b**) (700 mg, 2.057 mmol), benzaldehyde (627.33 μL, 654.93 mg, 6.171 mmol) and pyrrole (570.1 μL, 551.28 mg, 8.228 mmol) was refluxed in propionic acid (180 mL) for 2 h. The propionic acid was removed under reduced pressure and the crude product was purified on a basic alumina column by using hexanes/$CHCl_3$ 75:25 (87 mg, ~5%). ^{1}H NMR (400 MHz, $CDCl_3$, 25°C, TMS): δ = 8.93–8.79 (m, 8H, β-pyrrolic *H*), 8.29–8.16 (m, 6H, *o*-phenyl *H*), 7.82–7.67 (m, 11H, *m,p*-phenyl *H* (9H) and benzocrown-phenyl *H*(2H)), 7.18–7.13 (m, 1H, benzocrown-phenyl *H*), 4.42–4.33 (m, 2H, crownethylene *H*), 4.31–4.24 (m, 2H, crownethylene *H*), 4.11–4.03 (m, 2H, crownethylene *H*), 3.96–3.85 (m, 4H, crownethylene *H*), 3.83–3.72 (m, 10H, crownethylene *H*), −2.77 (br s, 2H, imino *H*); UV/Vis (toluene): λ_{max} = 421.5, 516.0, 550.5, 592.5, 652.0 nm.

5-(Benzo-[18]crown-6)-10,15,20-triphenylporphyrinatozinc(II) (2): The free-base porphyrin **2a** (50 mg, 0.059 mmol) was dissolved in $CHCl_3$ (10 ml), a saturated solution of zinc acetate in methanol was added to the solution, and the resulting mixture was refluxed for 2 h. The course of the reaction was followed spectrophotometrically by monitoring the disappearance of the 516 nm band of **2a**. At the end, the reaction mixture was washed with water and dried over anhydrous Na_2SO_4. Chromatography on basic alumina column by using hexanes/$CHCl_3$ 75:25 gave the title compound (49 mg, ~90%). ^{1}H NMR (400 MHz, $CDCl_3$, 25°C, TMS): δ = 8.98–8.87 (m, 8H, β-pyrrolic *H*), 8.24–8.17 (m, 6H, *o*-phenyl *H*), 7.79–7.66 (m, 11H, *m,p*-phenyl *H*(9H) and benzocrown-phenyl *H*-(2H)), 7.12–7.08 (m, 1H, benzocrown-phenyl *H*), 4.19–4.14 (m, 2H, crownethylene *H*), 4.06–3.98 (m, 2H, crownethylene *H*), 3.68–3.61 (m, 2H, crownethylene *H*), 3.58–3.40 (m, 14H, crownethylene *H*); UV/Vis

(toluene): λ_{max} = 424.0, 549.5, 589.5 nm; ESI mass in CH_2Cl_2: *m*/*z* (%): calcd: 912.37; found: 912.3 (57) $[M]^+$, 943.1 (100) $[M+MeOH]^+$.

H_2-5,10,15,20-Tetra-(benzo-[18]crown-6)-porphyrin (3a): This compound was prepared according to the reported procedures[27] for H_2-5,10,15,20-tetra(benzo-[15]crown-5)-porphyrin with some modifications. A mixture of 4′-formylbenzo-[18]crown-6 (**1b**) (502.3 mg, 1.5 mmol) and pyrrole (95 μL, 91.9 mg, 1.4 mmol) was refluxed in propionic acid (115 mL) for 3 h. The crude product was purified on a basic alumina column with chloroform (116 mg, ~5%). ^{1}H NMR (400 MHz, $CDCl_3$, 25°C, TMS): δ = 8.88 (s, 8H, β-pyrrolic *H*), 7.79–7.70 (m, 8H, benzocrown-phenyl *H*), 7.24–7.22 (m, 4H, benzocrown-phenyl *H*), 4.50–4.44 (m, 8H, crownethylene *H*), 4.33–4.27 (m, 8H, crownethylene *H*), 4.16–4.11 (m, 8H, crownethylene *H*), 4.01–3.90 (m, 16H, crownethylene *H*), 3.88–3.75 (m, 40H, crownethylene *H*), −2.79 (br s, 2H, imino *H*); UV/Vis (benzonitrile): λ_{max} = 429.5, 521.5, 559.0, 595.0, 655.0 nm.

5,10,15,20-Tetra(benzo-[18]crown-6)-porphyrinatozinc(II) (3): The free-base porphyrin **3a** (20 mg, 0.0129 mmol) was dissolved in $CHCl_3$ (10 mL), a saturated solution of zinc acetate in methanol was added to the solution, and the resulting mixture was refluxed for 2 h. The course of the reaction was followed spectrophotometrically by monitoring the disappearance of the 521 nm band of **3a**. At the end, the reaction mixture was washed with water and dried over anhydrous Na_2SO_4. Chromatography on silica gel column by using $CHCl_3$ gave the title compound (19 mg, ~90%). ^{1}H NMR (400 MHz, $CDCl_3$, 25°C, TMS): δ = 8.97 (s, 8H, β-pyrrolic *H*), 7.78–7.68 (m, 8H, benzocrown-phenyl *H*), 7.18 (d, 4H, benzocrown-phenyl *H*), 4.41–4.29 (m, 8H, crownethylene *H*), 4.26–4.10 (m, 8H, crownethylene*H*), 3.99–3.86 (m, 8H, crownethylene *H*), 3.85–3.54 (m, 56H, crownethylene *H*); UV/Vis (benzonitrile): λ_{max} = 434.5, 562.0, 604.5 nm; ESI mass in CH_2Cl_2: *m*/*z* (%):calcd: 1615.12; found: 1647.1 (100) $[M+MeOH]^+$.

2-(3′-Pyridyl)-5-(*n*-butylammonium)-3,4-fulleropyrrolidine (4): H-Lys-(Boc)-OH (100 mg, 0.406 mmol) and 3-pyridine carboxyaldehyde (76 μL) were added to a solution of C_{60} (100 mg, 0.138 mmol) in toluene, and refluxed for 3 h. The solvent was evaporated by vacuum, purified on silica gel by using toluene/ethyl acetate 8:2 to obtain N-Boc protected **4** (85 mg, 62%). Next, to a dichloromethane solution of N-Boc protected **4** (75 mg in 5 mL), trifluoroacetic acid (3 mL), and *m*-cresol (50 μL) was added and stirred for 3 h.[28] The solvent and acid were removed under vacuum and the solid product (66 mg, 97%) was washed in toluene several times to desired **4**. ^{1}H NMR (400 MHz, $CDCl_3$, 25°C, TMS): δ = 9.13, 8.60, 8.48, 7.64 (s, d, t, t, 4H, 3 pyridine *H*), 6.15, 5.17, 5. 14 (s, d, d, 3H, pyrrolidine *H*), 3.01–1.94 (d, m, m, m, 8H, -(CH_2)$_4$-); ESI mass in CH_2Cl_2: *m*/*z*: calcd: 912; found: 912.8; UV/Vis (MeOH): λ_{max} = 204, 254.5 nm.

2-Phenyl-5-(*n*-butylammonium)-3,4-fulleropyrrolidine (5): H-Lys(Boc)-OH (100 mg, 0.406 mmol) and benzaldehyde (72 μL) were added to a solution of C_{60} (100 mg, 0.138 mmol) in toluene (100 mL) and refluxed for 2 h. The solvent was evaporated by vacuum, purified on silica gel by using toluene/ethyl acetate 9:1 to obtain N-Boc protected **5** (93 mg, 68%). To unprotect the Boc group, to a dichloromethane solution (5 mL) of 2-phenyl-5-(4′-Boc-amino-*n*-butyl)-3,4-fulleropyrrolidine (82 mg), trifluoroacetic acid (3 mL) and *m*-cresol (50 μL) were added and stirred for 4 h. The solvent and acid were removed in vacuum and solid product was washed in toluene several times, yielding the desired product **5** (72 mg, 97%). ^{1}H NMR (400 MHz, $CDCl_3$, 25°C, TMS): δ = 7.3–7.77 (m, 5H, phenyl *H*), 6.0, 5.15, 5. 07 (s, d, d, 3H, pyrrolidine *H*), 3.01–1.94 (d, m, m, m, 8H, -(CH_2)$_4$-); ESI mass in CH_2Cl_2: *m*/*z*: calcd for: 911.0; found: 912.2; UV/Vis (MeOH): λ_{max} = 204, 254 nm.

Instrumentation: The UV/Vis spectral measurements were carried out with a Shimadzu Model 1600 UV/Vis spectrophotometer. The fluorescence emission was monitored by using a Spex Fluorolog-tau spectrometer. The ^{1}H NMR studies were carried out on a Varian 400 MHz spectrometer. Tetramethylsilane (TMS) was used as an internal standard. Cyclic voltammograms were recorded on an EG&G Model 263A potentiostat using a three electrode system. A platinum button or glassy carbon electrode was used as the working electrode. A platinum wire served as the counter electrode and a Ag/AgCl was used as the reference electrode. Ferrocene/ferrocenium redox couple was used as an internal standard. All the solutions were purged prior to electrochemical and spectral measurements using argon gas. The computational calculations were performed by ab initio B3LYP/3-21G(*) methods with GAUSSIAN 03 software package[29] on high speed computers. The images of the frontier orbitals were generated from Gauss View-03 software. The ESI-Mass spectral analyses of the newly synthesized compounds were performed by using a Finnigan LCQ-Deca mass spectrometer. For this, the compounds (about 0.1 mM) were prepared in CH_2Cl_2, freshly distilled over calcium hydride.

Time-resolved emission and transient absorption measurements: The picosecond time-resolved fluorescence spectra were measured by using an argon-ion pumped Ti/sapphire laser (Tsunami) and a streak scope (Hamamatsu Photonics). The details of the experimental setup are described elsewhere.[30] Nanosecond transient absorption spectra in the NIR region were measured by means of laser-flash photolysis; 532 nm light from a Nd/YAG laser was used as the exciting source and a Ge-avalanche-photodiode module was used for detecting the monitoring light from a pulsed Xe lamp as described in our previous report.[30]

Acknowledgment

The authors are thankful to the donors of the Petroleum Research Fund administered by the American Chemical Society and National Institutes of Health (GM 59038). This research was partially supported by a Grant-in-Aid for the COE project, and for Scientific Research on Primary Area (417) from the Ministry of Education, Science, Sport and Culture of Japan (to OI and YA) for support of this work.

[1] a) R. A. Marcus, N. Sutin, *Biochim. Biophys. Acta* **1985**, *811*, 265; b) R. A. Marcus, *Angew. Chem.* **1993**, *105*, 1161; *Angew. Chem. Int. Ed. Engl.* **1993**, *32*, 1111; c) M. Bixon, J. Jortner, *Adv. Chem. Phys.* **1999**, *106*, 35.

[2] a) J. R. Winkler, H. B. Gray, *Chem. Rev.* **1992**, *92*, 369; b) C. Kirmaier, D. Holton, in *The Photosynthetic Reaction Center*, *Vol. II* (Eds.: J. Deisenhofer, J. R. Norris), Academic Press, San Diego, **1993**, pp. 49–70.

[3] a) G. McLendon, R. Hake, *Chem. Rev.* **1992**, *92*, 481; b) I. R. Gould, S. Farid, *Acc. Chem. Res.* **1996**, *29*, 522; c) N. Mataga, H. Miyasaka, *Adv. Chem. Phys.* **1999**, *107*, 431; d) F. D. Lewis, R. L. Letsinger, M. R. Wasielewski, *Acc. Chem. Res.* **2001**, *34*, 159.

[4] a) J. R. Miller, L. T. Calcaterra, G. L. Closs, *J. Am. Chem. Soc.* **1984**, *106*, 3047; b) G. L. Closs, J. R. Miller, *Science* **1988**, *240*, 440; c) J. S. Connolly, J. R. Bolton, in *Photoinduced Electron Transfer* (Eds.: M. A. Fox, M. Chanon), Elsevier, Amsterdam, **1988**, Part D, pp. 303–393.

[5] a) M. R. Wasielewski, *Chem. Rev.* **1992**, *92*, 435; b) H. Kurreck, M. Huber, *Angew. Chem.* **1995**, *107*, 929; *Angew. Chem. Int. Ed. Engl.* **1995**, *34*, 849; c) D. Gust, T. A. Moore, A. L. Moore, *Acc. Chem. Res.* **2001**, *34*, 40.

[6] a) A. Harriman, J.-P. Sauvage, *Chem. Soc. Rev.* **1996**, *25*, 41; b) M.-J. Blanco, M. C. Jiménez, J.-C. Chambron, V. Heitz, M. Linke, J.-P. Sauvage, *Chem. Soc. Rev.* **1999**, *28*, 293; c) V. Balzani, A. Juris, M. Venturi, S. Campagna, S. Serroni, *Chem. Rev.* **1996**, *96*, 759; d) *Electron Transfer in Chemistry* (Ed.: V. Balzani), Wiley-VCH, Weinheim, **2001**.

[7] a) M. N. Paddon-Row, *Acc. Chem. Res.* **1994**, *27*, 18; b) J. W. Verhoeven, *Adv. Chem. Phys.* **1999**, *106*, 603; c) K. Maruyama, A. Osuka, N. Mataga, *Pure Appl. Chem.* **1994**, *66*, 867; d) A. Osuka, N. Mataga, T. Okada, *Pure Appl. Chem.* **1997**, *69*, 797.

[8] a) J. S. Sessler, B. Wang, S. L. Springs, C. T. Brown, in *Comprehensive Supramolecular Chemistry* (Eds.: J. L. Atwood, J. E. D. Davies, D. D. MacNicol, F. Vögtle), Chapter 9, Pergamon, **1996**; b) T. Hayashi, H. Ogoshi, *Chem. Soc. Rev.* **1997**, *26*, 355; c) M. W. Ward, *Chem. Soc. Rev.* **1997**, *26*, 365.

[9] a) *Introduction of Molecular Electronics* (Eds.: M. C. Petty, M. R. Bryce, D. Bloor), Oxford University Press, New York, **1995**; b) *Molecular Switches* (Ed.: B. L. Feringa), Wiley-VCH, Weinheim, **2001**.

[10] a) H. W. Kroto, J. R. Heath, S. C. O'Brien, R. F. Curl, R. E. Smalley, *Nature* **1985**, *318*, 162; b) W. Kratschmer, L. D. Lamb, F. Fostiropoulos, D. R. Huffman, *Nature* **1990**, *347*, 345; c) *Fullerene and Related Structures*, *Vol. 199* (Ed.: A. Hirsch), Springer, Berlin, **1999**.

[11] D. Gust, T. A. Moore in *The Porphyrin Handbook*, *Vol. 8* (Eds.: K. M. Kadish, K. M. Smith, R. Guilard), Academic Press, Burlington, MA, **2000**, pp. 153–190.

[12] a) H. Imahori, Y. Sakata, *Adv. Mater.* **1997**, *9*, 537; b) M. Prato, *J. Mater. Chem.* **1997**, *7*, 1097; c) N. Martín, L. Sánchez, B. Illescas, I. Pérez, *Chem. Rev.* **1998**, *98*, 2527; d) F. Diederich, M. Gómez-López, *Chem. Soc. Rev.* **1999**, *28*, 263; e) D. M. Guldi, *Chem. Commun.* **2000**, 321; f) D. M. Guldi, M. Prato, *Acc. Chem. Res.* **2000**, *33*, 695; g) D. M. Guldi, *Chem. Soc. Rev.* **2002**, *31*, 22; h) M. D. Meijer, G. P. M. van Klink, G. van Koten, *Coord. Chem. Rev.* **2002**, *230*, 141; i) M. E. El-Khouly, O. Ito, P. M. Smith, F. D'Souza, *J. Photochem. Photobiol. C* **2004**, *5*, 79; j) H. Imahori, S. Fukuzmi, *Adv. Funct. Mater.* **2004**, *14*, 525; k) F. D'Souza, O. Ito, *Coord. Chem. Rev.* **2005**, in press.

[13] a) H. Imahori, K. Hagiwara, T. Akiyama, M. Aoki, S. Taniguchi, T. Okada, M. Shirakawa, Y. Sakata, *Chem. Phys. Lett.* **1996**, *263*, 545; b) D. M. Guldi, K.-D. Asmus, *J. Am. Chem. Soc.* **1997**, *119*, 5744; c) H. Imahori, M. E. El-Khouly, M. Fujitsuka, O. Ito, Y. Sakata, S. Fukuzumi, *J. Phys. Chem. A* **2001**, *105*, 325.

[14] a) C. Luo, D. M. Guldi, H. Imahori, K. Tamaki, Y. Sakata, *J. Am. Chem. Soc.* **2000**, *122*, 6535; b) H. Imahori, D. M. Guldi, K. Tamaki, Y. Yoshida, C. Luo, Y. Sakata, S. Fukuzumi, *J. Am. Chem. Soc.* **2001**, *123*, 6617; c) H. Imahori, K. Tamaki, Y. Araki, Y. Sekiguchi, O. Ito, Y. Sakata, S. Fukuzumi, *J. Am. Chem. Soc.* **2002**, *124*, 5165; d) P. A. Liddell, G. Kodis, A. L. Moore, T. A. Moore, D. Gust, *J. Am. Chem. Soc.* **2002**, *124*, 7668; e) N. Watanabe, N. Kihara, Y. Furusho, T. Takata, Y. Araki, O. Ito, *Angew. Chem.* **2003**, *115*, 705; *Angew. Chem. Int. Ed.* **2003**, *42*, 681; f) K. Ohkubo, H. Kotani, J. Shao, Z. Ou, K. M. Kadish, G. Li, R. K. Pandey, M. Fujitsuka, O. Ito, H. Imahori, S. Fukuzumi, *Angew. Chem.* **2004**, *116*, 871; *Angew. Chem. Int. Ed.* **2004**, *43*, 853; g) G. de la Torre, F. Giacalone, J. L. Segura, N. Martin, D. M. Guldi, *Chem. Eur. J.* **2005**, *11*, 1267.

[15] a) N. V. Tkachenko, L. Rantala, A. Y. Tauber, J. Helaja, P. H. Hynninen, H. Lemmetyinen, *J. Am. Chem. Soc.* **1999**, *121*, 9378; b) V. Vehmanen, N. V. Tkachenko, A. Y. Tauber, P. H. Hynninen, H. Lemmetyinen, *Chem. Phys. Lett.* **2001**, *345*, 213; c) T. J. Kesti, N. V. Tkachenko, V. Vehmanen, H. Yamada, H. Imahori, S. Fukuzumi, H. Lemmetyinen, *J. Am. Chem. Soc.* **2002**, *124*, 8067; d) V. Vehmanen, N. V. Tkachenko, A. Efimov, P. Damlin, A. Ivaska, H. Lemmetyinen, *J. Phys. Chem. A* **2002**, *106*, 8029; e) N. V. Tkachenko, H. Lemmetyinen, J. Sonoda, K. Ohkubo, T. Sato, H. Imahori, S. Fukuzumi, *J. Phys. Chem. A* **2003**, *107*, 8834; f) V. Chukharev, N. V. Tkachenko, A. Efimov, D. M. Guldi, A. Hirsch, M. Scheloske, H. Lemmetyinen, *J. Phys. Chem. B* **2004**, *108*, 16377.

[16] a) H. Imahori, K. Hagiwara, M. Aoki, T. Akiyama, S. Taniguchi, T. Okada, M. Shirakawa, Y. Sakata, *J. Am. Chem. Soc.* **1996**, *118*, 11771; b) H. Imahori, Y. Mori, Y. Matano, *J. Photochem. Photobiol. C* **2003**, *4*, 51; c) D. Kuciauskas, S. Lin, G. R. Seely, A. L. Moore, T. A. Moore, D. Gust, T. Drovetskaya, C. A. Reed, P. D. W. Boyd, *J. Phys. Chem.* **1996**, *100*, 15926; d) F. D'Souza, S. Gadde, M. E. Zandler, K. Arkady, M. E. El-Khouly, M. Fujitsuka, O. Ito, *J. Phys. Chem. A* **2002**, *106*, 12393; e) F. D'Souza, G. R. Deviprasad, M. E. Zandler, M. E. El-Khouly, M. Fujitsuka, O. Ito, *J. Phys. Chem. B* **2002**, *106*, 4952.

[17] a) M. M. Olmstead, D. A. Costa, K. Maitra, B. C. Noll, S. L. Phillips, P. M. Van Calcar, A. L. Balch, *J. Am. Chem. Soc.* **1999**, *121*, 7090; b) P. D. W. Boyd, M. C. Hodgson, C. E. F. Richard, A. G. Oliver, L. Chaker, P. J. Brothers, R. D. Bolskar, F. S. Tham, C. A. Reed, *J. Am. Chem. Soc.* **1999**, *121*, 10487; c) D. R. Evans, N. L. P. Fackler, Z. Xie, C. E. F. Rickard, P. D. W. Boyd, C. A. Reed, *J. Am. Chem. Soc.* **1999**, *121*, 8466; d) Y. Sun, T. Drovetskaya, R. D. Bolskar, R. Bau, P. D. W. Boyd, C. A. Reed, *J. Org. Chem.* **1997**, *62*, 3642.

[18] a) E. Dietel, A. Hirsch, E. Eicchorn, A. Rieker, S. Hackbarth, B. Roder, *Chem. Commun.* **1998**, 1981; b) D. M. Guldi, C. Luo, M. Prato, A. Troisi, F. Zerbetto, M. Scheloske, E. Dietel, W. Bauer, A. Hirsch, *J. Am. Chem. Soc.* **2001**, *123*, 9166; c) D. I. Schuster, P. Cheng, S. R. Wilson, V. Prokhorenko, M. Katterle, A. R. Holzwarth, S. E. Braslavsky, G. Klihm, R. M. Williams, C. Luo, *J. Am. Chem. Soc.* **1999**, *121*, 11599.

[19] a) F. D'Souza, G. R. Deviprasad, M. E. El-Khouly, M. Fujitsuka, O. Ito, *J. Am. Chem. Soc.* **2001**, *123*, 5277; b) F. D'Souza, G. R. Deviprasad, M. E. Zandler, M. E. El-Khouly, M. Fujitsuka, O. Ito, *J. Phys. Chem. A* **2003**, *107*, 4801; c) F. D'Souza, S. Gadde, M. E. Zandler, M. Itou, Y. Araki, O. Ito, *Chem. Commun.* **2004**, 2276; d) F. D'Souza, R. Chitta, S. Gadde, M. E. Zandler, A. S. D. Sandanayaka, Y. Araki, O. Ito, *Chem. Commun.* **2005**, 1279.

[20] a) N. Solladie, M. E. Walther, M. Gross, T. M. F. Duarte, C. Bourgogne, J.-F. Nierengarten, *Chem. Commun.* **2003**, 2412; b) M. J. Gunter, *Eur. J. Org. Chem.* **2004**, 1655; c) Y. G. Gorbunova, L. A. Lapkina, A. Y. Tsivadze, *J. Coord. Chem.* **2003**, *56*, 1223; d) V. Balzani, A. Credi, M. Venturi, *Coord. Chem. Rev.* **1998**, *171*, 3; e) C. F. van Nostrum, R. J. M. Notle, *Chem. Commun.* **1996**, 2385; f) A. P. de Silva, H. Q. Nimal, N. Gunaratne, T. Gunnlaugsson, C. P. McCoy, P. R. S. Maxwell, J. T. Rademacher, R. E. Rice, *Pure Appl. Chem.* **1996**, *68*, 1443; g) J.-P. Sauvage, C. Dietrich-Buchecker, *Molecular Catenanes, Rotaxanes and Knots*, Wiley-VCH, Weinheim, Germany, **1999**; h) D. B. Amabilino, J. F. Stoddart, *Chem. Rev.* **1995**, *95*, 2725; i) T. J. Hubin, D. H. Busch, *Coord. Chem. Rev.* **2000**, *200*, 1172; j) F. Vögtle, T. Dunnwald, T. Schmidt, *Acc. Chem. Res.* **1996**, *29*, 451; k) A. S. D. Sandanayaka, N. Watanabe, K.-I. Ikeshita, Y. Araki, N. Kihara, Y. Furusho, O. Ito, T. Takata, *J. Phys. Chem. B* **2005**, *109*, 2516, and references therein.

[21] H. A. Benesi, J. H. Hildebrand, *J. Am. Chem. Soc.* **1949**, *71*, 2703.

[22] a) F. D'Souza, M. E. Zandler, P. M. Smith, G. R. Deviprasad, K. Arkady, M. Fujitsuka, O. Ito, *J. Phys. Chem. A* **2002**, *106*, 649; b) M. E. Zandler, P. M. Smith, M. Fujitsuka, O. Ito, F. D'Souza, *J. Org. Chem.* **2002**, *67*, 9122; c) F. D'Souza, G. R. Deviprasad, M. E. Zandler, V. T. Hoang, K. Arkady, M. VanStipdonk, A. Perera, M. E. El-Khouly, M. Fujitsuka, O. Ito, *J. Phys. Chem. A* **2002**, *106*, 3243; d) R. Marczak, V. T. Hoang, K. Noworyta, M. E. Zandler, W. Kutner, F. D'Souza, *J. Mater. Chem.* **2002**, *12*, 2123; e) M. E. El-Khouly, L. M. Rogers, M. E. Zandler, G. Suresh, M. Fujitsuka, O. Ito, F. D'Souza, *ChemPhysChem* **2003**, *4*, 474; f) F. D'Souza, P. M. Smith, M. E. Zandler, A. L. McCarty, M. Itou, Y. Araki, O. Ito, *J. Am. Chem. Soc.* **2004**, *126*, 7898; g) R. Chitta, L. M. Rogers, A. Wanklyn, P. A. Karr, P. K. Kahol, M. E. Zandler, F. D'Souza, *Inorg. Chem.* **2004**, *43*, 6969.

[23] a) D. Rehm, A. Weller, *Isr. J. Chem.* **1970**, *8*, 259; b) N. Mataga, H. Miyasaka, in *Electron Transfer* (Eds.: J. Jortner, M. Bixon), Wiley, New York, **1999**, Part 2, pp. 431–496.

[24] a) T. Nojiri, A. Watanabe, O. Ito, *J. Phys. Chem. A* **1998**, *102*, 5215; b) H. N. Ghosh, H. Pal, A. V. Sapre, J. P. Mittal, *J. Am. Chem. Soc.* **1993**, *115*, 11722; c) M. Fujitsuka, O. Ito, T. Yamashiro, Y. Aso, T. Otsubo, *J. Phys. Chem. A* **2000**, *104*, 4876.

[25] K. M. Smith, *Porphyrins and Metalloporphyrins*, Elsevier, New York, **1977**.

[26] P. K. Olga, G. K. Alexander, V. R. A. Elena, *Tetrahedron* **2003**, *59*, 231.

[27] V. Thanabal, V. Krishnan, *J. Am. Chem. Soc.* **1982**, *104*, 3643.

[28] F. Pellarini, D. Pantarotto, T. Da Ros, A. Giangaspero, A. Tossi, M. Prato, *Org. Lett.* **2001**, *3*, 1845.

[29] *Gaussian 03* (Revision B-04), M. J. Frisch, G. W. Trucks, H. B. Schlegel, G. E. Scuseria, M. A. Robb, J. R. Cheeseman, J. A. Montgomery, Jr., T. Vreven, K. N. Kudin, J. C. Burant, J. M. Millam, S. S. Iyengar, J. Tomasi, V. Barone, B. Mennucci, M. Cossi, G. Scalmani, N. Rega, G. A. Petersson, H. Nakatsuji, M. Hada, M. Ehara, K. Toyota, R. Fukuda, J. Hasegawa, M. Ishida, T. Nakajima, Y. Honda, O. Kitao, H. Nakai, M. Klene, X. Li, J. E. Knox, H. P. Hratchian, J. B. Cross, C. Adamo, J. Jaramillo, R. Gomperts, R. E. Stratmann, O. Yazyev, A. J. Austin, R. Cammi, C. Pomelli, J. W. Ochterski, P. Y. Ayala, K. Morokuma, G. A. Voth, P. Salvador, J. J. Dannenberg,

V. G. Zakrzewski, S. Dapprich, A. D. Daniels, M. C. Strain, O. Farkas, D. K. Malick, A. D. Rabuck, K. Raghavachari, J. B. Foresman, J. V. Ortiz, Q. Cui, A. G. Baboul, S. Clifford, J. Cioslowski, B. B. Stefanov, G. Liu, A. Liashenko, P. Piskorz, I. Komaromi, R. L. Martin, D. J. Fox, T. Keith, M. A. Al-Laham, C. Y. Peng, A. Nanayakkara, M. Challacombe, P. M. W. Gill, B. Johnson, W. Chen, M. W. Wong, C. Gonzalez, J. A. Pople, Gaussian, Inc., Pittsburgh PA, **2003**.

[30] a) K. Matsumoto, M. Fujitsuka, T. Sato, S. Onodera, O. Ito, *J. Phys. Chem. B* **2000**, *104*, 11632; b) S. Komamine, M. Fujitsuka, O. Ito, K. Morikawa, T. Miyata, T. Ohno, *J. Phys. Chem. A* **2000**, *104*, 11497; c) M. Yamazaki, Y. Araki, M. Fujitsuka, O. Ito, *J. Phys. Chem. A* **2001**, *105*, 8615.

Received: February 21, 2005
Published online: May 10, 2005